# ENERGY LEVELS, WAVELENGTHS, AND TRANSITION PROBABILITIES OF INTERCOMBINATION LINES IN THE SPECTRA OF Ge-LIKE I, Cs, AND La IONS[**]

**L. H. Hao[*], X. P. Kang, J. J. Liu**

*School of Electronic Communication Engineering, Hainan Tropical Ocean University, Sanya, Hainan, 572022, China; e-mail: lhhao_1020@163.com*

*Energy levels, wavelengths, transition probabilities, and line strengths are calculated for the allowed electric dipole $4s^2 4p^2$–$4s4p^3$ and $4s^2 4p^2$–$4s^2 4p4d$ transitions of Ge-like ions with Z = 53, 55 and 57, I XXII, Cs XXIV, and La XXVI. By employing active-space techniques to expand the configuration list, we also include the Breit interaction and quantum electrodynamical (QED) effects to correct the atomic state wave functions and the corresponding energies. Both valence correlation and core polarization effects are included. The results are compared with the available experimental and other theoretical results.*

***Keywords:*** *energy level, wavelength, valance-valence correlation.*

# УРОВНИ ЭНЕРГИИ, ДЛИНЫ ВОЛН И ВЕРОЯТНОСТИ ПЕРЕХОДОВ ИНТЕРКОМБИНАЦИОННЫХ ЛИНИЙ В СПЕКТРАХ Ge-ПОДОБНЫХ ИОНОВ I, Cs и La

**L. H. Hao[*], X. P. Kang, J. J. Liu**

*Школа электронной инженерии связи, Хайнаньский университет тропического океана, Санья, Хайнань, 572022, Китай; e-mail: lhhao_1020@163.com*

*Рассчитаны уровни энергии, длины волн, вероятности переходов, уширение линий для разрешенных дипольных переходов $4s^2 4p^2$–$4s4p^3$ и $4s^2 4p^2$–$4s^2 4p4d$ в Ge-подобных ионах I XXII, Cs XXIV и La XXVI с Z = 53, 55 и 57. С использованием методов активного пространства для расширения списка конфигурации учтены взаимодействие Брейта и квантовые электродинамические эффекты для коррекции волновых функций атомного состояния и соответствующих энергий, а также валентная корреляция и эффекты поляризации ядра. Результаты сопоставлены с имеющимися экспериментальными и теоретическими данными.*

***Ключевые слова:*** *уровень энергии, длина волны, валентно-валентная корреляция.*

**Introduction.** Theoretical predictions of the atomic characteristics for multi-valence-electron ions have progressed in accuracy during the past few years, and their quality, in many cases, is now comparable to that for one-valence electron ions [1]. For Ge-like ions with $70 \le Z \le 92$, the theoretical energy level, wavelengths, and transition probabilities of the $4s^2 4p^2$, $4s4p^3$, and $4s^2 4p4d$ states were calculated using the fully relativistic multiconfiguration Dirac–Fock method (MCDF) by Palmeri et al. [2]. The transition energy, oscillator strength, and transition probability for $4s$–$4p$ of Cu, Zn, Ga, and Ge-like gold ions were calculated using the fully relativistic MCDF method by Bian et al. [3]. The energy levels and lifetimes of the low-lying excited states within the $n = 4$ complex were reported for Ni- to Kr-like Pt ions using the relativistic multi-reference Møller–Plesset many-body perturbation theory by Santana et al. [4]. The complete energy level spectra were calculated for the $4s^2 4p^N$, $4s4p^{N+1}$, and $4s^2 4p^{N-1}4d$ configurations of the tungsten ions from $W^{43+}$ to $W^{38+}$ using the *ab initio* quasirelativistic Hartree-Fock approximation by Bogdanovich et al. [5]. The

atomic structure and X-ray spectra of Ge-like through V-like W ions were calculated using the flexible atomic code (FAC) by Clementson et al. [6]. The energy levels, wavelengths, transition probabilities, and oscillator strengths for Ge-like Kr, Mo, Sn, and Xe ions were calculated using the fully relativistic MCDF method by Nagy and El-sayed [7]. The energies of the low-lying levels, transition energies, and rates of the ground state transitions in Cu- through Ge-like ions of iodine were calculated using the fully relativistic MCDF method by Li et al. [8]. The relativistic multireference Møller–Plesset second-order perturbation theory calculations were performed for the ground and low-lying excited states of the $4s^24p^2$ configuration in germanium and Ge-like ions, $As^{1+}$, $Se^{2+}$, $Br^{3+}$, and $Kr^{4+}$ by Ishikawa and Vilkas [9]. Transition probabilities for the $4s^24p^2$–$4s4p^3$ transitions of Ge-like ions with $37 \leq Z \leq 47$ were studied using the relativistic Hartree–Fock method by Biémont et al. [10]. The energy levels, wavelengths, oscillator strengths, and radiative electric dipole (E1) and magnetic quadrupole (M2) transition probabilities for Ge-like ions with $49 \leq Z \leq 58$ among the lowest 88 fine structure levels belonging to the $([Ar]3d^{10})4s^24p^2$, $([Ar]3d^{10})4s^24p4d$, $([Ar]3d^{10})4s4p^3$, $([Ar]3d^{10})$ $4s4p^24d$, $([Ar]3d^{10})4s^24d^2$, and $([Ar]3d^{10})4p^4$ configurations were calculated using the fully relativistic multiconfiguration Dirac–Fock (MCDF) approach by Chen and Wang [11]. The atomic data and spectral line intensities for highly ionized tungsten (Co-like $W^{47+}$ to Rb-like $W^{37+}$) in a high-temperature, low-density plasma were calculated using the fully relativistic *ab initio* calculations by Fournier [12].

The experimental measurements of a large number of energy levels are available; for example, the electron-beam ion-trap (EBIT) spectra of tungsten in the extreme-ultraviolet (EUV) were recorded by Utter et al. [13]. Spectra of $W^{39+}$–$W^{47+}$ in the 12–20 nm region were observed with an electron beam ion trap light source by Ralchenko et al. [14]. Lines of the resonance transition array $4s^24p^2$–$4s4p^3$ in the Ge-like ions Ru XIII-Cd XVII were identified in the spectra emitted from laser-produced plasmas by Litzén and Zeng [15]. The spectrum of krypton ionized four times (KrV) in the vacuum-ultraviolet region (432–2000 Å) for $4s^24p^2$, $4s4p^3$, and $4s^24p4d$ configurations were observed with a FTHETA-pinch light source by Trigueiros et al. [16]. Identifications of strong $n = 4 - n = 4$ transitions from Rb-like hafnium (35+) to Co-like gold (52+) were determined with the aid of collisional-radiative modelling of the EBIT plasma by Draganić et al. [17]. EUV spectroscopy of highly charged Rb-like $Xe^{17+}$ to Cu-like $Xe^{25+}$ ions were investigated with the Berlin EBIT by Biedermann et al. [18]. Also, EUV spectra of Sn XIX to Sn XXII were measured in low-density and high-temperature plasmas produced in the Large Helical Device at the National Institute for Fusion Science by Suzuki et al. [19]. In addition, the spectral data of some ions for highly ionized atoms (Ti, V, Cr, Mn, Fe, Co, Ni, Cu, Kr, and Mo) were compiled by Shirai et al. [20]. However, the data of theoretical and experimental investigation of the radiative parameters of highly charged ions of the germanium isoelectronic sequence are still extremely fragmentary.

The purpose of the present paper is to fill in this gap. In this paper, we calculate energy levels, wavelengths, transition probabilities and line strengths for electric dipole transitions among the levels belonging to the $4s^24p^2$, $4s4p^3$, and $4s^24p4d$ states for Ge-like I, Cs, and La ions using the full relativistic multiconfiguration Dirac–Hartree–Fock (MCDHF) method.

**Computational procedure.** The energy levels, wavelengths, transition probabilities and line strengths for the $4s^24p^2$–$4s4p^3$ and $4s^24p^2$–$4s^24p4d$ electric dipole (E1) transitions are calculated for Ge-like ions from $Z = 53$, 55 and 57, I XXII, Cs XXIV, and La XXVI. The calculations are performed using the fully relativistic multiconfiguration Dirac–Hartree–Fock (MCDHF) approach with the MCDFGME program [21, 22] of Desclaux and Indelicato.

All odd and even configurations within the $n = 4$ layer are included in the calculations. These configurations are $4s^24p^2$, $4s^24d^2$, $4s^24p4f$, $4s^24f^2$, $4s4p^24d$, $4s4p4d4f$, $4p^4$, $4p^24d^2$, $4p^24f^2$ and $4s^24p4d$, $4s^24d4f$, $4s4p^3$, $4s4p^24f$, $4s4p4d^2$, $4s4p4f^2$, $4s4d^24f$, $4p^34d$, $4p^24d4f$, $4p4d^3$ for the even and odd configurations, respectively. The MCDHF calculations are completed with the inclusion of the relativistic two-body Breit interaction and of the quantum electrodynamic corrections (QED), which arise due to self-energy and vacuum polarization.

We make two calculations, one with the valance-valence (VV) correlation and one including the core-valance (CV) correlation of $3d$. The electron configuration can be defined as the ground state $1s^22s^22p^63s^23p^63d^{10}4s^24p^2$ and the excited state $1s^22s^22p^63s^23p^63d^{10}4s4p^3$ and $1s^22s^22p^63s^23p^63d^{10}4s^24p4d$. In this situation, $4s^24p^2$, $4s4p^3$, and $4s^24p4d$ are valence electrons and $1s^22s^22p^63s^23p^63d^{10}$ is core electrons. Two kinds of the model can be expressed:

$$\text{VV model: } 1s^22s^22p^63s^23p^63d^{10}n_1l_1n_2l_2n_3l_3n_4l_4,$$
$$\text{CV model: } 1s^22s^22p^63s^23p^63d^{10}n_1l_1n_2l_2n_3l_3n_4l_4n_5l_5.$$

We gradually increase the principal quantum number $n$. It is convenient to refer to the $\{1s, 2s, 2p, \ldots, 4s, 4p, 4d, 4f\}$ set of orbitals as the $n = 4$ orbital layer and $\{1s, 2s, 2p, \ldots, 5s, 5p, 5d, 5f, 5g\}$ as $n = 5$. In order to avoid confusion of the configuration, we only calculate $n = 5$ orbital layer.

**Results and discussion.** In relativistic calculations such as those of the MCDHF method, energy levels are classified by $J$ and $\pi$. States with the same $J^{\pi}$ are further classified by ordering their total energies. For convenience, however, we assign the more familiar spectroscopic notations $(^{2s+1}L)$ to label each level. Thus, for example, the second $J^{\pi} = 2^{+}$ state for Ge-like ions is termed $(4s^{2}4p^{2})^{1}D_{2}$. We use the $J^{\pi}$ classification when ambiguity arises in assigning the $SL$ quantum numbers.

To assist readers in identifying energy levels and locating transitions, we present schematic diagrams of energy levels, with their labels, for Ge-like ions in Fig. 1. The relative positions of energy levels in these figures resemble those in the actual spectra of heavy ions, although some of these levels are rearranged as $Z$ increases along isoelectronic sequences.
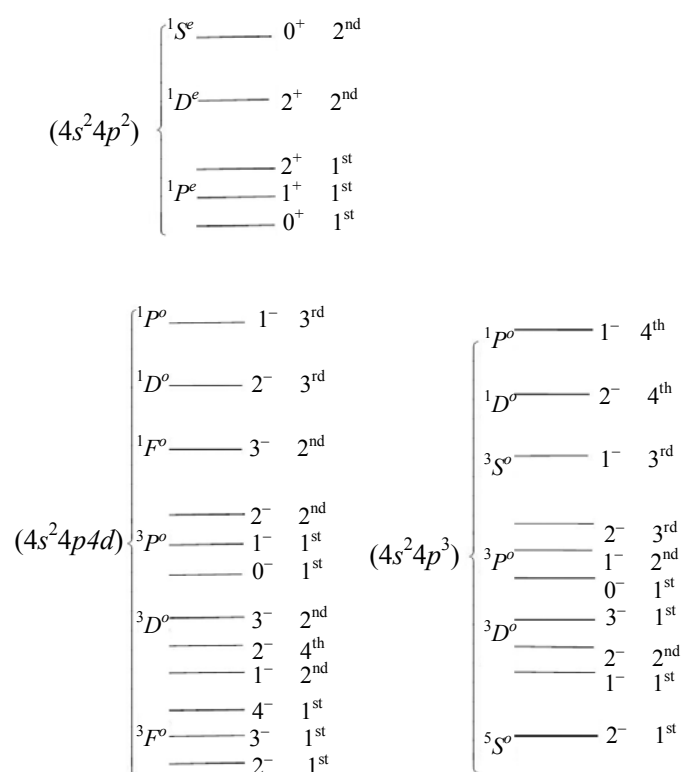


Fig. 1. Shematic diagram of energy levels for Ge-like ions.

*Energy levels.* The calculated MCDHF results for I XXII are compared with the results of the multiconfiguration Dirac–Fock [8, 11] methods, as listed in Table 1, where each level is presented in both the LS-coupling and the *jj*-coupling schemes. The comparison shows that the MCDHF energy levels are in excellent agreement (within ≤0.71%) with the MCDF results [8]. As can be seen in Table 1, our results are also in good agreement with the MCDF results of Chen and Wang [11], the difference being 0.07–8.00% for most cases. However, a more detailed comparison of the calculated energies for these transitions (Table 1) indicates that some splitting energies given by Li et al. [8] calculations are in better agreement with the MCDF results of Chen and Wang [11] than our MCDHF results. This may be because we have include a limited number of configurations in our calculation. The deviations between the present values and the other theoretical data suggest that additional correlation effects must be taken into account to reduce the discrepancy. The MCDHF energy level values for the $4s^{2}4p^{2}$, $4s4p^{3}$, and $4s^{2}4p4d$ configurations for Ge-like Cs XXIV and La XXVI are listed in Tables 2 and 3. In Tables 2 and 3, our results show excellent agreement with the MCDF values of Chen and Wang [11] (0.09% and 1.41%). These calculations provide a theoretical benchmark for comparison with experiment and theory.

TABLE 1. MCDHF Energy Levels (in cm$^{-1}$) of $4s^2 4p^2$, $4s4p^3$, and $4s^2 4p 4d$ Configurations for I XXII

| Index | $jj$-coupling | $J$ | $(LS)^p$ | MCDHF | MCDF [8] | MCDF [11] |
|---|---|---|---|---|---|---|
| 1 | $4s^2 4p^{*2}$ | 0 | $^3P_0^e$ | 0 | 0 | 0 |
| 2 | $4s^2 4p^* 4p$ | 1 | $^3P_1^e$ | 99435 | 99588 | 99364 |
| 3 | $4s^2 4p^* 4p$ | 2 | $^3P_2^e$ | 119227 | 118986 | 118991 |
| 4 | $4s^2 4p^2$ | 2 | $^1D_2^e$ | 234105 | 233527 | 233448 |
| 5 | $4s^2 4p^2$ | 0 | $^1S_0^e$ | 282332 | 280332 | 280681 |
| 6 | $4s4p^{*2}4p$ | 2 | $^5S_2^o$ | 471665 | 470345 | 469416 |
| 7 | $4s4p^{*2}4p$ | 1 | $^3D_1^o$ | 545266 | 544715 | 543814 |
| 8 | $4s4p^2 4p^*$ | 2 | $^3D_2^o$ | 578809 | 577001 | 575963 |
| 9 | $4s4p^2 4p^*$ | 3 | $^3D_3^o$ | 610694 | 608885 | 607860 |
| 10 | $4s4p^2 4p^*$ | 0 | $^3P_0^o$ | 652189 | 650180 | 649580 |
| 11 | $4s4p^2 4p^*$ | 1 | $^3P_1^o$ | 665690 | 664854 | 664100 |
| 12 | $4s4p^3$ | 2 | $^3P_2^o$ | 672024 | 671051 | 669728 |
| 13 | $4s4p^2 4p^*$ | 1 | $^3S_1^o$ | 718592 | 720469 | 719975 |
| 14 | $4s4p^2 4p^*$ | 2 | $^1D_2^o$ | 756136 | 755105 | 753098 |
| 15 | $4s4p^3$ | 1 | $^1P_1^o$ | 841786 | 844997 | 842326 |
| 16 | $4s^2 4p^* 4d^*$ | 2 | $^3F_2^o$ | 779255 | | 782270 |
| 17 | $4s^2 4p^* 4d$ | 3 | $^3F_3^o$ | 823353 | | 821251 |
| 18 | $4s^2 4p 4d^*$ | 2 | $^3P_2^o$ | 847099 | | 848662 |
| 19 | $4s^2 4p 4d^*$ | 1 | $^3D_1^o$ | 857883 | | 858561 |
| 20 | $4s^2 4p 4d$ | 4 | $^3F_4^o$ | 913303 | | 907724 |
| 21 | $4s^2 4p 4d$ | 2 | $^1D_2^o$ | 942678 | | 935969 |
| 22 | $4s^2 4p 4d^*$ | 0 | $^3P_0^o$ | 949149 | | 946002 |
| 23 | $4s^2 4p 4d^*$ | 3 | $^3D_3^o$ | 957366 | | 954316 |
| 24 | $4s^2 4p^* 4d^*$ | 1 | $^3P_1^o$ | 963053 | | 956225 |
| 25 | $4s^2 4p^* 4d$ | 2 | $^3D_2^o$ | 979576 | | 971340 |
| 26 | $4s^2 4p 4d$ | 3 | $^1F_3^o$ | 1022105 | | 1019923 |
| 27 | $4s^2 4p 4d$ | 1 | $^1P_1^o$ | 1042442 | | 1035149 |

TABLE 2. MCDHF Energy Levels (in cm$^{-1}$) of $4s^2 4p^2$, $4s4p^3$, and $4s^2 4p 4d$ Configurations for Cs XXIV

| Index | $jj$-coupling | $J$ | $(LS)^p$ | MCDHF | MCDF [11] |
|---|---|---|---|---|---|
| 1 | $4s^2 4p^{*2}$ | 0 | $^3P_0^e$ | 0 | 0 |
| 2 | $4s^2 4p^* 4p$ | 1 | $^3P_1^e$ | 126765 | 126648 |
| 3 | $4s^2 4p^* 4p$ | 2 | $^3P_2^e$ | 148175 | 147896 |
| 4 | $4s^2 4p^2$ | 2 | $^1D_2^e$ | 291428 | 290678 |
| 5 | $4s^2 4p^2$ | 0 | $^3S_0^e$ | 342398 | 340671 |
| 6 | $4s4p^{*2}4p$ | 2 | $^5S_2^o$ | 535636 | 533408 |
| 7 | $4s4p^{*2}4p$ | 1 | $^3D_1^o$ | 613065 | 611876 |
| 8 | $4s4p^2 4p^*$ | 2 | $^3D_2^o$ | 663588 | 660572 |
| 9 | $4s4p^2 4p^*$ | 3 | $^3D_3^o$ | 700400 | 697440 |
| 10 | $4s4p^2 4p^*$ | 0 | $^3P_0^o$ | 744615 | 741916 |
| 11 | $4s4p^2 4p^*$ | 1 | $^3P_1^o$ | 760825 | 759395 |
| 12 | $4s4p^3$ | 2 | $^1D_2^o$ | 765354 | 762623 |
| 13 | $4s4p^2 4p^*$ | 1 | $^3S_1^o$ | 812156 | 813302 |
| 14 | $4s4p^2 4p^*$ | 2 | $^3P_2^o$ | 856335 | 852930 |
| 15 | $4s4p^3$ | 1 | $^1P_1^o$ | 967178 | 968809 |
| 16 | $4s^2 4p^* 4d^*$ | 2 | $^3F_2^o$ | 885953 | 883899 |
| 17 | $4s^2 4p^* 4d$ | 3 | $^3F_3^o$ | 921453 | 914889 |
| 18 | $4s^2 4p 4d^*$ | 2 | $^3P_2^o$ | 949649 | 941644 |
| 19 | $4s^2 4p 4d^*$ | 1 | $^3D_1^o$ | 945679 | 943202 |
| 20 | $4s^2 4p 4d$ | 4 | $^3F_4^o$ | 1030238 | 1025253 |
| 21 | $4s^2 4p^* 4d^*$ | 2 | $^1D_2^e$ | 1048567 | 1050643 |
| 22 | $4s^2 4p 4d^*$ | 0 | $^3P_0^o$ | 1066178 | 1061268 |
| 23 | $4s^2 4p 4d^*$ | 1 | $^3P_1^o$ | 1067923 | 1073974 |
| 24 | $4s^2 4p^* 4d^*$ | 3 | $^3D_3^o$ | 1075059 | 1069337 |

*Continue Table 2*

| Index | *jj*-coupling | $J$ | $(LS)^p$ | MCDHF | MCDF [11] |
|---|---|---|---|---|---|
| 25 | $4s^24p^*4d$ | 2 | $^3D_2^o$ | 1115275 | 1093053 |
| 26 | $4s^24p4d$ | 3 | $^1F_3^o$ | 1145035 | 1142398 |
| 27 | $4s^24p4d$ | 1 | $^1P_1^o$ | 1176849 | 1160236 |

TABLE 3. MCDHF Energy Levels (in cm$^{-1}$) of $4s^24p^2$, $4s4p^3$, and $4s^24p4d$ Configurations for La XXVI

| Index | *jj*-coupling | $J$ | $(LS)^p$ | MCDHF | MCDF [11] |
|---|---|---|---|---|---|
| 1 | $4s^24p^{*2}$ | 0 | $^3P_0^e$ | 0 | 0 |
| 2 | $4s^24p^*4p$ | 1 | $^3P_1^e$ | 159150 | 158917 |
| 3 | $4s^24p^*4p$ | 2 | $^3P_2^e$ | 182148 | 181800 |
| 4 | $4s^24p^2$ | 2 | $^1D_2^e$ | 358864 | 357960 |
| 5 | $4s^24p^2$ | 0 | $^1S_0^e$ | 412567 | 410831 |
| 6 | $4s4p^{*2}4p$ | 2 | $^5S_2^o$ | 604910 | 602730 |
| 7 | $4s4p^{*2}4p$ | 1 | $^3D_1^o$ | 686386 | 685665 |
| 8 | $4s4p^24p^*$ | 2 | $^3D_2^o$ | 759026 | 755795 |
| 9 | $4s4p^24p^*$ | 3 | $^3D_2^o$ | 800518 | 797462 |
| 10 | $4s4p^24p^*$ | 0 | $^3P_0^o$ | 847533 | 844907 |
| 11 | $4s4p^24p^*$ | 2 | $^3D_2^o$ | 866458 | 863898 |
| 12 | $4s4p^3$ | 1 | $^3P_1^o$ | 867538 | 865337 |
| 13 | $4s^24p^24p^*$ | 1 | $^3S_1^o$ | 912061 | 917234 |
| 14 | $4s4p^24p^*$ | 2 | $^3P_2^o$ | 1015214 | 1010022 |
| 15 | $4s4p^3$ | 1 | $^1P_1^o$ | 1101985 | 1103742 |
| 16 | $4s^24p^*4d^*$ | 2 | $^3F_2^o$ | 950707 | 949488 |
| 17 | $4s^24p^*4d$ | 3 | $^3F_3^o$ | 1016589 | 1015052 |
| 18 | $4s^24p4d^*$ | 1 | $^3D_1^o$ | 1040050 | 1039237 |
| 19 | $4s^24p4d^*$ | 2 | $^3P_2^o$ | 1045555 | 1042183 |
| 20 | $4s^24p4d$ | 4 | $^3F_4^o$ | 1154173 | 1153997 |
| 21 | $4s^24p^*4d^*$ | 2 | $^3D_2^o$ | 1177057 | 1175524 |
| 22 | $4s^24p4d^*$ | 0 | $^3P_0^o$ | 1190490 | 1186658 |
| 23 | $4s^24p4d^*$ | 3 | $^3D_3^o$ | 1193158 | 1194404 |
| 24 | $4s^24p^*4d^*$ | 1 | $^3P_1^o$ | 1199639 | 1203017 |
| 25 | $4s^24p^*4d$ | 2 | $^3D_2^o$ | 1252477 | 1226576 |
| 26 | $4s^24p4d$ | 3 | $^1F_3^o$ | 1278741 | 1275969 |
| 27 | $4s^24p4d$ | 1 | $^1P_1^o$ | 1316082 | 1296913 |

*Wavelengths, transition probabilities, and line strengths.* Tables 4–6 contain the list of wavelengths (Å), transition probabilities in the length and velocity gauges (s$^{-1}$), and line strengths in the length gauge (a.u.) for electric dipole $4s^24p^2$–$4s4p^3$ and $4s^24p^2$–$4s^24p4d$ transitions. For strong transitions, the difference between transition probabilities in the Babushkin (length) and the Coulomb (velocity) gauges is within ~3% for all Ge-like ions with $Z = 53$, 55, and 57. This gives a clear indication of the accuracy of the results.

TABLE 4. Wavelengths, Transition Probabilities, and Line Strengths for Lines of I XXII.
The Notation a (b) Abbreviates a×10$^b$

| Lower | Upper | $\lambda$, Å | $A_L$, s$^{-1}$ | $A_V$, s$^{-1}$ | $S_L$ |
|---|---|---|---|---|---|
| $4s^24p^2\,{}^3P_0^e$ | $4s4p^3\,{}^3D_1^o$ | 183.40 | 2.54(10) | 2.59(10) | 2.32(–1) |
| | $4s4p^3\,{}^3P_1^o$ | 150.22 | 5.46(9) | 5.42(9) | 2.74(–2) |
| | $4s4p^3\,{}^3S_1^o$ | 139.94 | 2.23(10) | 2.19(10) | 7.96(–2) |
| | $4s4p^3\,{}^1P_1^o$ | 118.79 | 6.02(10) | 5.99(10) | 3.45(–2) |
| | $4s^24p4d\,{}^3D_1^o$ | 116.57 | 2.74(11) | 2.68(11) | 6.42(–1) |
| | $4s^24p4d\,{}^3P_1^o$ | 103.84 | 5.08(8) | 4.96(8) | 8.42(–4) |
| | $4s^24p4d\,{}^1P_1^o$ | 95.93 | 1.78(9) | 1.82(9) | 2.33(–3) |
| $4s^24p^2$ | $4s4p^3\,{}^3D_1^o$ | 380.32 | 4.36(7) | 3.46(7) | 2.74(–3) |
| | $4s4p^3\,{}^3P_1^o$ | 260.85 | 9.86(8) | 1.01(9) | 2.59(–2) |
| | $4s4p^3\,{}^3S_1^o$ | 228.34 | 2.68(9) | 2.76(9) | 4.92(–2) |

*Continue Table 4*

| Lower | Upper | $\lambda$, Å | $A_L$, s$^{-1}$ | $A_V$, s$^{-1}$ | $S_L$ |
|---|---|---|---|---|---|
| | $4s4p^3\,^1P_1^o$ | 178.74 | 2.09(10) | 2.15(10) | 1.77(−1) |
| | $4s^24p4d\,^3D_1^o$ | 174.07 | 1.15(9) | 1.08(9) | 1.12(−2) |
| | $4s^24p4d\,^1P_1^o$ | 131.74 | 2.35(11) | 2.29(11) | 7.88(−1) |
| $4s^24p^2\,^3P_1^e$ | $4s4p^3\,^3P_0^o$ | 180.91 | 2.70(10) | 2.74(10) | 7.88(−2) |
| | $4s4p^3\,^3D_1^o$ | 224.30 | 2.32(8) | 2.25(8) | 3.87(−3) |
| | $4s4p^3\,^3P_1^o$ | 176.60 | 3.47(10) | 3.50(10) | 2.83(−1) |
| | $4s4p^3\,^3S_1^o$ | 162.56 | 3.14(10) | 3.12(10) | 1.99(−1) |
| | $4s4p^3\,^1P_1^o$ | 134.71 | 1.46(10) | 1.39(10) | 8.89(−2) |
| | $4s4p^3\,^3S_2^o$ | 269.65 | 1.64(9) | 1.70(9) | 7.82(−2) |
| | $4s4p^3\,^3D_2^o$ | 208.61 | 8.95(9) | 9.12(9) | 2.00(−1) |
| | $4s4p^3\,^1D_2^o$ | 174.65 | 4.37(8) | 4.38(8) | 5.75(−3) |
| | $4s4p^3\,^3P_2^o$ | 151.58 | 4.75(8) | 5.72(8) | 4.94(−3) |
| | $4s^24p4d\,^3P_0^o$ | 117.67 | 2.29(11) | 2.26(11) | 1.84(−1) |
| | $4s^24p4d\,^3D_1^o$ | 131.83 | 6.01(10) | 5.97(10) | 6.83(−2) |
| | $4s^24p4d\,^3P_1^o$ | 115.76 | 1.29(11) | 1.25(11) | 2.90(−1) |
| | $4s^24p4d\,^1P_1^o$ | 106.03 | 6.17(9) | 6.12(9) | 1.08(−2) |
| | $4s^24p4d\,^3F_2^o$ | 147.07 | 6.25(9) | 6.20(9) | 1.12(−2) |
| | $4s^24p4d\,^3P_2^o$ | 132.96 | 1.20(11) | 1.18(11) | 6.82(−1) |
| | $4s^24p4d\,^1D_2^o$ | 118.57 | 1.33(11) | 1.30(11) | 5.29(−1) |
| | $4s^24p4d\,^3D_2^o$ | 113.60 | 2.78(10) | 2.74(10) | 6.26(−2) |
| $4s^24p^2\,^1D_2^e$ | $4s4p^3\,^3D_1^o$ | 234.72 | 3.29(9) | 3.29(9) | 6.31(−2) |
| | $4s4p^3\,^3P_1^o$ | 183.00 | 1.15(9) | 1.21(9) | 5.31(−3) |
| | $4s4p^3\,^3S_1^o$ | 167.96 | 9.59(10) | 9.54(10) | 6.72(−1) |
| | $4s4p^3\,^1P_1^o$ | 138.40 | 3.43(9) | 3.35(9) | 6.79(−3) |
| | $4s4p^3\,^3S_2^o$ | 283.74 | 1.01(9) | 1.06(9) | 5.69(−2) |
| | $4s4p^3\,^3D_2^o$ | 217.59 | 3.43(8) | 3.49(8) | 8.71(−3) |
| | $4s4p^3\,^1D_2^o$ | 180.90 | 3.69(10) | 3.74(10) | 5.38(−1) |
| | $4s4p^3\,^3D_3^o$ | 203.47 | 5.34(9) | 5.41(9) | 1.56(−1) |
| | $4s^24p4d\,^3D_1^o$ | 135.47 | 2.15(9) | 1.98(9) | 3.05(−2) |
| | $4s^24p4d\,^3P_1^o$ | 118.58 | 4.15(10) | 3.97(10) | 1.02(−1) |
| | $4s^24p4d\,^1P_1^o$ | 108.38 | 3.18(7) | 3.25(7) | 3.89(−5) |
| | $4s^24p4d\,^3F_2^o$ | 151.63 | 2.12(10) | 2.08(10) | 1.88(−1) |
| | $4s^24p4d\,^3P_2^o$ | 136.62 | 6.69(10) | 6.51(10) | 4.20(−1) |
| | $4s^24p4d\,^1D_2^o$ | 121.52 | 1.46(11) | 1.37(11) | 6.42(−1) |
| | $4s^24p4d\,^3D_2^o$ | 116.30 | 3.26(10) | 3.20(10) | 7.61(−2) |
| | $4s^24p4d\,^3F_3^o$ | 141.52 | 3.38(10) | 3.27(10) | 3.31(−1) |
| | $4s^24p4d\,^3D_3^o$ | 119.39 | 2.71(11) | 2.69(11) | 1.58(0) |
| | $4s^24p4d\,^1F_3^o$ | 110.82 | 5.99(10) | 6.00(10) | 2.35(−1) |
| $4s^24p^2\,^3P_2^e$ | $4s4p^3\,^3D_1^o$ | 321.38 | 2.99(8) | 3.01(8) | 1.32(−2) |
| | $4s4p^3\,^3P_1^o$ | 231.70 | 2.67(8) | 2.65(8) | 6.71(−3) |
| | $4s4p^3\,^3S_1^o$ | 205.12 | 2.88(9) | 2.90(9) | 3.84(−2) |
| | $4s4p^3\,^1P_1^o$ | 164.56 | 8.21(10) | 8.17(10) | 6.07(−1) |
| | $4s4p^3\,^3S_2^o$ | 422.95 | 2.98(7) | 2.85(7) | 5.26(−3) |
| | $4s4p^3\,^3D_2^o$ | 290.10 | 2.35(8) | 2.42(8) | 1.42(−2) |
| | $4s4p^3\,^1D_2^o$ | 228.35 | 2.32(9) | 2.32(9) | 6.81(−2) |
| | $4s4p^3\,^3P_2^o$ | 192.46 | 1.56(10) | 1.51(10) | 3.52(−1) |
| | $4s4p^3\,^3D_3^o$ | 266.54 | 3.15(9) | 3.16(9) | 2.03(−1) |
| | $4s^24p4d\,^3P_1^o$ | 137.32 | 6.12(10) | 5.89(10) | 3.19(−1) |
| | $4s^24p4d\,^1P_1^o$ | 123.82 | 1.99(7) | 1.93(7) | 3.37(−3) |
| | $4s^24p4d\,^3F_2^o$ | 183.68 | 1.65(10) | 1.66(10) | 2.53(−4) |
| | $4s^24p4d\,^1D_2^o$ | 141.27 | 1.41(10) | 1.33(10) | 9.80(−2) |
| | $4s^24p4d\,^3D_2^o$ | 134.27 | 1.92(11) | 1.86(11) | 1.14(0) |
| | $4s^24p4d\,^3D_3^o$ | 138.40 | 2.51(10) | 2.46(10) | 2.29(−1) |
| | $4s^24p4d\,^1F_3^o$ | 127.02 | 2.56(11) | 2.53(11) | 1.82(0) |

TABLE 5. Wavelengths, Transition Probabilities, and Line Strengths for Lines of Cs XXIV.
The Notation a (b) Abbreviates $a \times 10^b$

| Lower | Upper | $\lambda$, Å | $A_L$, s$^{-1}$ | $A_V$, s$^{-1}$ | $S_L$ |
|---|---|---|---|---|---|
| $4s^24p^2\,{}^3P_0^e$ | $4s4p^3\,{}^3D_1^o$ | 163.11 | 3.38(10) | 3.41(10) | 2.17(−1) |
| | $4s4p^3\,{}^3P_1^o$ | 131.44 | 7.46(9) | 7.39(9) | 2.50(−2) |
| | $4s4p^3\,{}^3S_1^o$ | 123.74 | 2.34(10) | 2.30(10) | 6.58(−2) |
| | $4s4p^3\,{}^1P_1^o$ | 103.39 | 1.96(10) | 1.92(10) | 9.76(−2) |
| | $4s^24p4d\,{}^3D_1^o$ | 105.64 | 3.11(11) | 3.13(11) | 4.76(−1) |
| | $4s^24p4d\,{}^3P_1^o$ | 95.37 | 5.80(8) | 5.72(8) | 1.13(−3) |
| | $4s^24p4d\,{}^1P_1^o$ | 84.97 | 1.89(9) | 1.84(9) | 1.72(−3) |
| $4s^24p^2\,{}^1S_0^e$ | $4s4p^3\,{}^3D_1^o$ | 369.46 | 3.05(7) | 3.10(7) | 2.28(−3) |
| | $4s4p^3\,{}^3P_1^o$ | 238.99 | 1.30(9) | 1.34(9) | 2.62(−2) |
| | $4s4p^3\,{}^3S_1^o$ | 212.70 | 3.18(9) | 3.28(9) | 4.66(−2) |
| | $4s4p^3\,{}^1P_1^o$ | 160.06 | 1.61(10) | 1.63(10) | 9.77(−2) |
| | $4s^24p4d\,{}^3D_1^o$ | 164.25 | 2.45(9) | 2.55(9) | 9.32(−3) |
| | $4s^24p4d\,{}^3P_1^o$ | 135.76 | 1.23(9) | 1.37(9) | 2.63(−2) |
| | $4s^24p4d\,{}^1P_1^o$ | 121.94 | 3.09(11) | 3.09(11) | 7.89(−1) |
| $4s^24p^2\,{}^3P_1^e$ | $4s4p^3\,{}^3P_0^o$ | 161.85 | 3.37(10) | 3.42(10) | 7.06(−2) |
| | $4s4p^3\,{}^3D_1^o$ | 205.63 | 5.36(8) | 5.28(8) | 6.90(−3) |
| | $4s4p^3\,{}^3P_1^o$ | 157.71 | 4.59(10) | 4.63(10) | 2.67(−1) |
| | $4s4p^3\,{}^3S_1^o$ | 146.59 | 3.43(10) | 3.42(10) | 1.61(−1) |
| | $4s4p^3\,{}^1P_1^o$ | 118.99 | 8.00(10) | 7.84(10) | 1.99(−1) |
| | $4s4p^3\,{}^3S_2^o$ | 244.58 | 2.35(9) | 2.40(9) | 8.49(−2) |
| | $4s4p^3\,{}^3D_2^o$ | 186.28 | 1.01(10) | 1.05(10) | 1.61(−1) |
| | $4s4p^3\,{}^1D_2^o$ | 156.60 | 7.88(8) | 7.93(8) | 7.47(−3) |
| | $4s4p^3\,{}^3P_2^o$ | 137.14 | 7.40(8) | 7.35(8) | 4.12(−2) |
| | $4s^24p4d\,{}^3P_0^o$ | 106.22 | 2.94(11) | 2.97(11) | 1.74(−1) |
| | $4s^24p4d\,{}^3P_1^o$ | 121.60 | 1.39(10) | 1.38(10) | 1.40(−1) |
| | $4s^24p4d\,{}^3P_1^o$ | 106.45 | 2.09(11) | 2.19(11) | 4.70(−1) |
| | $4s^24p4d\,{}^1P_1^o$ | 95.20 | 7.52(9) | 7.64(9) | 8.33(−3) |
| | $4s^24p4d\,{}^3F_2^o$ | 131.15 | 1.20(10) | 1.17(10) | 6.69(−2) |
| | $4s^24p4d\,{}^3P_2^o$ | 121.48 | 1.23(11) | 1.25(11) | 5.44(−1) |
| | $4s^24p4d\,{}^1D_2^o$ | 107.42 | 1.64(11) | 1.65(11) | 4.87(−1) |
| | $4s^24p4d\,{}^3D_2^o$ | 102.13 | 2.02(10) | 2.01(10) | 2.60(−2) |
| $4s^24p^2\,{}^1D_2^e$ | $4s4p^3\,{}^3D_1^o$ | 215.10 | 4.86(9) | 4.88(9) | 7.16(−2) |
| | $4s4p^3\,{}^3P_1^o$ | 163.23 | 1.40(9) | 1.48(9) | 3.48(−3) |
| | $4s4p^3\,{}^3S_1^o$ | 151.52 | 1.13(11) | 1.12(11) | 5.80(−1) |
| | $4s4p^3\,{}^1P_1^o$ | 122.10 | 5.81(8) | 5.90(8) | 7.57(−5) |
| | $4s4p^3\,{}^3S_2^o$ | 258.09 | 1.46(9) | 1.50(9) | 6.18(−2) |
| | $4s4p^3\,{}^3D_2^o$ | 194.02 | 3.95(8) | 4.02(8) | 7.12(−3) |
| | $4s4p^3\,{}^1D_2^o$ | 162.03 | 4.34(10) | 4.40(10) | 4.56(−1) |
| | $4s4p^3\,{}^3P_2^o$ | 140.92 | 2.09(10) | 2.06(10) | 1.26(−1) |
| | $4s4p^3\,{}^3D_3^o$ | 181.09 | 6.28(9) | 6.35(9) | 1.29(−1) |
| | $4s^24p4d\,{}^3D_1^o$ | 124.88 | 8.16(9) | 7.98(9) | 9.09(−2) |
| | $4s^24p4d\,{}^3P_1^o$ | 108.10 | 4.71(10) | 4.68(10) | 3.48(−2) |
| | $4s^24p4d\,{}^3F_2^o$ | 135.04 | 1.25(10) | 1.30(10) | 2.58(−1) |
| | $4s^24p4d\,{}^3P_2^o$ | 124.81 | 7.94(10) | 8.11(10) | 2.37(−1) |
| | $4s^24p4d\,{}^1D_2^o$ | 109.97 | 1.44(11) | 1.48(11) | 7.79(−1) |
| | $4s^24p4d\,{}^3D_2^o$ | 104.43 | 3.17(10) | 3.13(10) | 9.20(−3) |
| | $4s^24p4d\,{}^3F_3^o$ | 129.37 | 4.88(10) | 4.88(10) | 3.65(−1) |
| | $4s^24p4d\,{}^3D_3^o$ | 107.92 | 3.36(11) | 3.37(11) | 1.46(0) |
| | $4s^24p4d\,{}^1F_3^o$ | 100.34 | 6.29(10) | 6.27(10) | 1.50(−1) |
| $4s^24p^2\,{}^3P_2^e$ | $4s4p^3\,{}^3D_1^o$ | 310.91 | 2.42(8) | 2.43(8) | 1.08(−2) |
| | $4s4p^3\,{}^3P_1^o$ | 213.04 | 7.25(8) | 7.15(8) | 1.19(−2) |
| | $4s4p^3\,{}^3S_1^o$ | 191.53 | 3.56(9) | 3.57(9) | 3.81(−2) |
| | $4s4p^3\,{}^1P_1^o$ | 147.98 | 9.75(10) | 9.70(10) | 4.68(−1) |
| | $4s4p^3\,{}^3S_2^o$ | 410.49 | 2.44(7) | 2.52(7) | 4.14(−3) |

*Continue Table 5*

| Lower | Upper | λ, Å | $A_L$, s$^{-1}$ | $A_V$, s$^{-1}$ | $S_L$ |
|---|---|---|---|---|---|
| | $4s4p^3\ ^3D_2^o$ | 269.70 | 3.21(8) | 3.24(8) | 1.54(−2) |
| | $4s4p^3\ ^1D_2^o$ | 211.00 | 3.17(9) | 3.19(9) | 7.35(−2) |
| | $4s4p^3\ ^3P_2^o$ | 177.25 | 1.70(9) | 1.75(9) | 3.47(−1) |
| | $4s4p^3\ ^3D_3^o$ | 244.52 | 3.77(9) | 4.00(9) | 1.90(−1) |
| | $4s^24p4d\ ^3P_1^o$ | 128.14 | 7.12(10) | 7.14(10) | 1.75(−1) |
| | $4s^24p4d\ ^1P_1^o$ | 114.99 | 1.37(8) | 1.37(8) | 4.63(−2) |
| | $4s^24p4d\ ^3F_2^o$ | 167.46 | 2.95(9) | 3.03(9) | 3.35(−2) |
| | $4s^24p4d\ ^3P_2^o$ | 152.01 | 5.58(9) | 5.44(9) | 2.13(−3) |
| | $4s^24p4d\ ^1D_2^o$ | 130.13 | 1.43(10) | 1.42(10) | 4.12(−2) |
| | $4s^24p4d\ ^3D_2^o$ | 123.43 | 2.90(11) | 3.00(11) | 1.29(0) |
| | $4s^24p4d\ ^3F_3^o$ | 159.81 | 5.25(8) | 5.35(8) | 1.11(−2) |
| | $4s^24p4d\ ^3D_3^o$ | 127.67 | 2.40(10) | 2.42(10) | 1.73(−1) |
| | $4s^24p4d\ ^1F_3^o$ | 117.20 | 3.13(11) | 3.13(11) | 1.74(0) |

TABLE 6. Wavelengths, Transition Probabilities, and Line Strengths for Lines of La XXVI.
The Notation a (b) Abbreviates a×10$^b$

| Lower | Upper | λ, Å | $A_L$, s$^{-1}$ | $A_V$, s$^{-1}$ | $S_L$ |
|---|---|---|---|---|---|
| $4s^24p^2\ ^3P_0^e$ | $4s4p^3\ ^3D_1^o$ | 145.69 | 4.44(10) | 4.52(10) | 2.03(−1) |
| | $4s4p^3\ ^3P_1^o$ | 115.41 | 1.07(10) | 1.05(10) | 2.44(−2) |
| | $4s4p^3\ ^3S_1^o$ | 109.64 | 2.93(10) | 2.88(10) | 5.72(−2) |
| | $4s4p^3\ ^1P_1^o$ | 90.75 | 2.30(9) | 2.36(9) | 2.55(−3) |
| | $4s^24p4d\ ^3D_1^o$ | 95.78 | 3.47(11) | 3.51(11) | 3.11(−1) |
| | $4s^24p4d\ ^3D_1^o$ | 84.96 | 3.24(8) | 3.27(8) | 4.75(−4) |
| | $4s^24p4d\ ^1P_1^o$ | 76.98 | 1.93(9) | 1.99(9) | 1.19(−3) |
| $4s^24p^2\ ^1S_0^e$ | $4s4p^3\ ^3D_1^o$ | 364.20 | 3.27(7) | 3.27(7) | 1.85(−3) |
| | $4s4p^3\ ^3P_1^o$ | 220.32 | 1.64(9) | 1.70(9) | 2.60(−2) |
| | $4s4p^3\ ^3S_1^o$ | 200.20 | 3.74(9) | 3.77(9) | 4.44(−2) |
| | $4s4p^3\ ^1P_1^o$ | 145.05 | 2.41(10) | 2.47(10) | 1.09(−1) |
| | $4s^24p4d\ ^3D_1^o$ | 158.82 | 1.97(9) | 2.07(9) | 1.15(−2) |
| | $4s^24p4d\ ^3P_1^o$ | 128.93 | 2.76(9) | 2.86(9) | 1.62(−2) |
| | $4s^24p4d\ ^1P_1^o$ | 111.77 | 2.52(11) | 3.55(11) | 7.09(−1) |
| $4s^24p^2\ ^3P_1^e$ | $4s4p^3\ ^3P_0^o$ | 145.27 | 4.20(10) | 4.25(10) | 6.36(−2) |
| | $4s4p^3\ ^3D_1^o$ | 189.67 | 9.71(8) | 9.68(8) | 9.81(−3) |
| | $4s4p^3\ ^3P_1^o$ | 141.38 | 5.99(10) | 6.04(10) | 2.51(−1) |
| | $4s4p^3\ ^3S_1^o$ | 132.82 | 3.66(10) | 3.65(10) | 1.27(−1) |
| | $4s4p^3\ ^1P_1^o$ | 106.06 | 9.81(10) | 9.75(10) | 1.38(−1) |
| | $4s4p^3\ ^3S_2^o$ | 224.34 | 3.17(9) | 3.26(9) | 8.84(−2) |
| | $4s4p^3\ ^3D_2^o$ | 166.70 | 1.13(10) | 1.17(10) | 1.29(−1) |
| | $4s4p^3\ ^1D_2^o$ | 141.17 | 1.20(9) | 1.21(9) | 8.30(−3) |
| | $4s4p^3\ ^3P_2^o$ | 116.81 | 2.39(10) | 2.38(10) | 5.51(−2) |
| | $4s^24p4d\ ^3P_0^o$ | 96.68 | 3.44(11) | 3.49(11) | 1.54(−1) |
| | $4s^24p4d\ ^3D_1^o$ | 112.58 | 3.68(10) | 3.69(10) | 1.85(−1) |
| | $4s^24p4d\ ^3P_1^o$ | 96.21 | 1.95(11) | 1.97(11) | 4.72(−1) |
| | $4s^24p4d\ ^1P_1^o$ | 86.41 | 8.44(9) | 8.56(9) | 7.11(−3) |
| | $4s^24p4d\ ^3F_2^o$ | 126.78 | 3.54(9) | 3.39(9) | 2.00(−4) |
| | $4s^24p4d\ ^3P_2^o$ | 116.52 | 2.76(10) | 2.81(10) | 6.05(−1) |
| | $4s^24p4d\ ^3D_2^o$ | 97.93 | 1.90(11) | 1.92(11) | 4.27(−1) |
| | $4s^24p4d\ ^1D_2^o$ | 92.44 | 2.56(10) | 2.55(10) | 1.80(−2) |
| $4s^24p^2\ ^1D_2^e$ | $4s4p^3\ ^3D_1^o$ | 198.32 | 6.79(9) | 6.83(9) | 7.84(−2) |
| | $4s4p^3\ ^3P_1^o$ | 146.13 | 1.52(9) | 1.52(9) | 2.09(−3) |
| | $4s4p^3\ ^3S_1^o$ | 137.00 | 1.32(11) | 1.32(11) | 5.02(−1) |
| | $4s4p^3\ ^1P_1^o$ | 108.72 | 3.56(9) | 3.48(9) | 4.98(−3) |
| | $4s4p^3\ ^5S_2^o$ | 236.54 | 2.00(9) | 2.10(9) | 6.53(−2) |
| | $4s4p^3\ ^3D_2^o$ | 173.35 | 4.25(8) | 4.31(8) | 5.47(−3) |
| | $4s4p^3\ ^1D_2^o$ | 145.90 | 4.75(10) | 4.81(10) | 3.64(−1) |

*Continue Table 6*

| Lower | Upper | $\lambda$, Å | $A_L$, s$^{-1}$ | $A_V$, s$^{-1}$ | $S_L$ |
|---|---|---|---|---|---|
| | $4s4p^3\ ^3P_2^o$ | 120.04 | 1.40(9) | 1.30(9) | 2.31(−2) |
| | $4s4p^3\ ^3D_3^o$ | 161.72 | 7.29(9) | 7.38(9) | 1.06(−1) |
| | $4s^24p4d\ ^3P_2^o$ | 115.60 | 9.89(9) | 9.79(9) | 1.53(−1) |
| | $4s^24p4d\ ^3P_1^o$ | 100.54 | 5.84(10) | 5.78(10) | 4.28(−2) |
| | $4s^24p4d\ ^3F_2^o$ | 130.01 | 4.49(10) | 4.39(10) | 9.30(−3) |
| | $4s^24p4d\ ^3D_2^o$ | 99.20 | 1.87(11) | 1.94(11) | 6.91(−1) |
| | $4s^24p4d\ ^1D_2^o$ | 93.46 | 2.01(10) | 1.96(10) | 4.04(−3) |
| | $4s^24p4d\ ^3F_3^o$ | 119.03 | 6.59(10) | 6.64(10) | 3.83(−1) |
| | $4s^24p4d\ ^3D_3^o$ | 98.30 | 3.86(11) | 3.90(11) | 1.27(0) |
| | $4s^24p4d\ ^1F_3^o$ | 91.22 | 6.21(10) | 6.19(10) | 1.10(−1) |
| $4s^24p^2\ ^3P_2^e$ | $4s4p^3\ ^3D_1^o$ | 305.32 | 2.05(8) | 2.04(8) | 8.63(−3) |
| | $4s4p^3\ ^3P_1^o$ | 197.01 | 1.48(9) | 1.43(9) | 1.67(−2) |
| | $4s4p^3\ ^3S_1^o$ | 180.77 | 4.19(9) | 4.23(9) | 3.67(−2) |
| | $4s4p^3\ ^1P_1^o$ | 134.57 | 1.26(11) | 1.25(11) | 4.53(−1) |
| | $4s4p^3\ ^5S_2^o$ | 407.43 | 2.13(7) | 2.21(7) | 3.49(−3) |
| | $4s4p^3\ ^3D_2^o$ | 250.90 | 4.26(8) | 4.36(8) | 1.64(−2) |
| | $4s4p^3\ ^1D_2^o$ | 196.59 | 3.86(9) | 3.90(9) | 7.24(−2) |
| | $4s4p^3\ ^3P_2^o$ | 152.36 | 2.49(10) | 2.52(10) | 3.05(−1) |
| | $4s4p^3\ ^3D_3^o$ | 226.42 | 4.42(9) | 4.53(9) | 1.77(−1) |
| | $4s^24p4d\ ^3D_1^o$ | 145.72 | 1.28(7) | 1.44(9) | 1.76(−2) |
| | $4s^24p4d\ ^3P_1^o$ | 120.28 | 1.22(10) | 1.32(10) | 8.72(−2) |
| | $4s^24p4d\ ^1P_1^o$ | 105.51 | 5.14(8) | 5.03(8) | 6.30(−2) |
| | $4s^24p4d\ ^3F_2^o$ | 170.06 | 2.16(8) | 2.18(8) | 1.64(−2) |
| | $4s^24p4d\ ^3P_2^o$ | 145.61 | 1.76(10) | 1.82(10) | 1.27(−2) |
| | $4s^24p4d\ ^3D_2^o$ | 121.30 | 9.27(9) | 9.31(9) | 2.32(−2) |
| | $4s^24p4d\ ^1D_2^o$ | 114.95 | 2.37(11) | 2.41(11) | 1.17(0) |
| | $4s^24p4d\ ^3F_3^o$ | 150.75 | 7.33(8) | 7.39(8) | 1.54(−2) |
| | $4s^24p4d\ ^3D_3^o$ | 118.98 | 2.16(10) | 2.22(10) | 1.26(−1) |
| | $4s^24p4d\ ^1F_3^o$ | 108.76 | 3.52(11) | 3.54(11) | 1.57(0) |
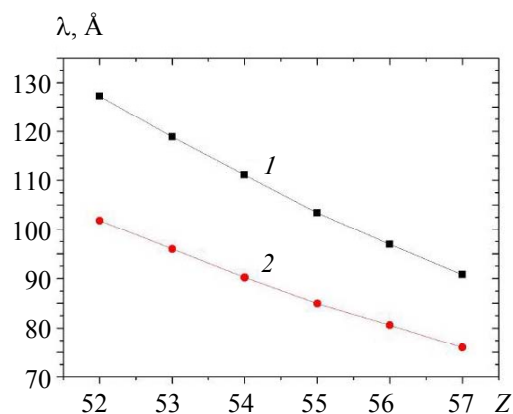


Fig. 2. MCDHF wavelenghts of the $4s^24p^2\ ^3P_0^e$–$4s4p^3\ ^1P_1^0$ (1) and of the $4s^24p^2\ ^3P_0^e$–$4s^24p4d\ ^1P_1^0$ transition (2) as a function of the atomic number Z.

In Fig. 2, the MCDHF wavelengths of both $4s^24p^2\ ^3P_0^e$–$4s4p^3\ ^1P_1^0$ and $4s^24p^2\ ^3P_0^e$–$4s^24p4d\ ^1P_1^0$ resonance transitions are plotted as a function of the atomic number from $Z = 52$ to $Z = 57$, showing two smooth trends. From the table entries, one can see that the wavelengths are monotonically decreasing with increasing $Z$.

Table 7 presents a comparison between the calculated MCDHF wavelengths and transition probabilities ($n = 5$) with other available theoretical results [8] for I XXII ions. This comparison shows an excellent agreement (within 1.31% for wavelengths and 20% for transition probabilities). The MCDHF wavelengths are in excellent agreement with the available experimental results of Träbert [23] (0.13% and 0.97%). As can be seen from Table 7, the contributions to the wavelengths of the configurations with $n = 5$ are small (~0.3%).

TABLE 7. Wavelengths and Transition Probabilities for Lines Of I XXII. Comparison with Theoretical [8] and Experimental [22] Measurements. The Notation a (b) Abbreviates $a \times 10^b$

| Lower | Upper | $\lambda$, Å | $A_L$, s⁻¹ | $\lambda$, Å | $A_L$, s⁻¹ | $\lambda$, Å | $A_L$, s⁻¹ | Experiment |
|---|---|---|---|---|---|---|---|---|
| | | Present ($n = 4$) | | Present ($n = 5$) | | Theory ($n = 4$) [8] | | [22] |
| $4s^24p^{2\ 3}P_0^e$ | $4s4p^{3\ 3}D_1^o$ | 183.5 | 2.44(10) | 183.40 | 2.54(10) | 183.6 | 2.53(10) | |
| | $4s4p^{3\ 3}P_1^o$ | 150.37 | 5.46(9) | 150.22 | 5.46(9) | 150.4 | 5.38(9) | |
| | $4s4p^{3\ 3}S_1^o$ | 139.79 | 2.11(10) | 139.94 | 2.23(10) | 138.8 | 2.38(10) | |
| | $4s4p^{3\ 1}P_1^o$ | 118.74 | 2.94(10) | 118.79 | 3.02(10) | 118.3 | 3.08(10) | |
| $4s^24p^{2\ 3}S_0^e$ | $4s4p^{3\ 3}D_1^o$ | 380.96 | 4.19(7) | 380.32 | 4.36(7) | 378.2 | 4.43(7) | |
| | $4s4p^{3\ 3}P_1^o$ | 261.47 | 9.64(8) | 260.85 | 9.86(8) | 260.1 | 1.08(9) | |
| | $4s4p^{3\ 3}S_1^o$ | 231.05 | 2.63(9) | 228.34 | 2.68(9) | 227.2 | 2.75(9) | |
| | $4s4p^{3\ 1}P_1^o$ | 178.69 | 2.05(10) | 178.74 | 2.09(10) | 177.1 | 2.03(10) | |
| $4s^24p^{2\ 3}P_1^e$ | $4s4p^{3\ 3}P_0^o$ | 181.03 | 2.60(10) | 180.91 | 2.70(10) | 181.6 | 2.80(10) | |
| | $4s4p^{3\ 3}D_1^o$ | 224.14 | 2.40(8) | 224.30 | 2.32(8) | 224.7 | 2.02(8) | |
| | $4s4p^{3\ 3}P_1^o$ | 176.65 | 3.33(10) | 176.60 | 3.47(10) | 176.9 | 3.27(10) | |
| | $4s4p^{3\ 3}S_1^o$ | 162.22 | 3.17(10) | 162.56 | 3.14(10) | 161.1 | 3.64(10) | |
| | $4s4p^{3\ 1}P_1^o$ | 134.54 | 2.49(10) | 134.71 | 2.46(10) | 134.2 | 2.30(10) | |
| | $4s4p^{3\ 5}S_2^o$ | 269.27 | 1.55(9) | 269.65 | 1.64(9) | 269.7 | 1.68(9) | 270.00±0.1 |
| | $4s4p^{3\ 3}D_2^o$ | 208.74 | 8.69(9) | 208.61 | 8.95(9) | 209.5 | 8.87(9) | |
| | $4s4p^{3\ 3}P_2^o$ | 174.67 | 4.32(8) | 174.65 | 4.37(8) | 175.0 | 4.15(8) | |
| | $4s4p^{3\ 1}D_2^o$ | 151.74 | 5.02(8) | 151.58 | 4.75(8) | 152.6 | 4.24(8) | |
| $4s^24p^{2\ 1}D_2^e$ | $4s4p^{3\ 3}D_1^o$ | 235.07 | 3.19(9) | 234.72 | 3.29(9) | 234.9 | 3.17(9) | |
| | $4s4p^{3\ 3}P_1^o$ | 183.37 | 1.29(9) | 183.00 | 1.15(9) | 183.2 | 1.25(9) | |
| | $4s4p^{3\ 3}S_1^o$ | 167.87 | 9.62(10) | 167.96 | 9.59(10) | 166.3 | 1.06(11) | |
| | $4s4p^{3\ 1}P_1^o$ | 138.40 | 2.41(9) | 138.40 | 2.43(9) | 137.7 | 2.62(9) | |
| | $4s4p^{3\ 5}S_2^o$ | 284.21 | 9.63(8) | 283.74 | 1.01(9) | 284.6 | 1.04(9) | 281.7±0.15 |
| | $4s4p^{3\ 3}D_2^o$ | 218.19 | 3.51(8) | 217.59 | 3.43(8) | 218.3 | 3.28(8) | |
| | $4s4p^{3\ 3}P_2^o$ | 181.24 | 3.50(10) | 180.90 | 3.69(10) | 190.5 | 3.55(10) | |
| | $4s4p^{3\ 3}D_3$ | 203.82 | 5.21(9) | 203.47 | 5.34(9) | 204.1 | 5.16(9) | |
| $4s^24p^{2\ 3}P_2^e$ | $4s4p^{3\ 3}D_1^o$ | 321.72 | 2.81(8) | 321.38 | 2.99(8) | 321.3 | 3.15(8) | |
| | $4s4p^{3\ 3}P_1^o$ | 232.13 | 3.04(8) | 231.70 | 2.67(8) | 231.8 | 2.47(8) | |
| | $4s4p^{3\ 3}S_1^o$ | 207.84 | 2.69(9) | 205.12 | 2.88(9) | 205.4 | 2.65(9) | |
| | $4s4p^{3\ 1}P_1^o$ | 164.48 | 9.12(10) | 164.56 | 9.21(10) | 163.5 | 9.17(10) | |
| | $4s4p^{3\ 5}S_2^o$ | 422.63 | 2.37(7) | 422.95 | 2.98(7) | 422.3 | 3.10(7) | |
| | $4s4p^{3\ 3}D_2^o$ | 290.92 | 2.23(8) | 290.10 | 2.35(8) | 291.1 | 2.15(8) | |
| | $4s4p^{3\ 3}P_2^o$ | 228.74 | 2.34(9) | 228.35 | 2.32(9) | 228.6 | 2.01(9) | |
| | $4s4p^{3\ 1}D_2^o$ | 190.94 | 1.95(10) | 192.46 | 1.56(10) | 191.7 | 1.66(10) | |
| | $4s4p^{3\ 3}D_3^o$ | 265.91 | 3.02(9) | 266.54 | 3.15(9) | 266.4 | 3.16(9) | |

**Conclusion.** The energy levels, wavelengths, transition probabilities, and line strengths are calculated for the allowed electric dipole ($E1$) $4s^24p^2$–$4s4p^3$ and $4s^24p^2$–$4s^24p4d$ transitions for Ge-like ions with $Z = 53$, 55, and 57. The calculations are performed using the multiconfiguration Dirac–Hartree-Fock (MCDHF) method, taking into account the correlations within the $n = 5$ complex and the quantum electrodynamic effects. A comparison between the MCDHF results of energy levels and wavelengths with the available experimental and other theoretical results shows excellent agreement. We report new data on the theoretical energies, wavelengths, transition probabilities, and line strengths of $4s^24p^2$, $4s4p^3$, and $4s^24p4d$ configurations for the allowed transitions in highly charged Ge-like I XXII, Cs XXIV, and La XXVI among these configurations.

**REFERENCES**

1. M. J. Vilkas, Y. Ishikawa, *Phys. Rev. A*, **72**, 032512 (2005).
2. P. Palmeri, P. Quinet, É. Biémont, E. Träbert, *At. Data Nucl. Data Tables*, **93**, 355–374 (2007).
3. G.-J. Bian, F. He, G. Jiang, Q.-P. Fan, F. Hu, *Phys. Scr.*, **90**, 015403 (2015).

4. J. A. Santana, Y. Ishikawa, E. Träbert, *At. Data Nucl. Data Tables,* **100**,183–271 (2014).

5. P. Bogdanovich, R. Karpuškienė, R. Kisielius, *Lith. J. Phys.*, **55**, 162–173 (2015).

6. J. Clementson, P. Beiersdorfer, T. Brage, M. F. Gu, *At. Data Nucl. Data Tables*, **100**, 577–649 (2014).

7. O. Nagy, F. El-Sayed, *At. Data Nucl. Data Tables*, **98**, 373–390 (2012).

8. J.-G. Li, E. Träbert, C.-Z. Dong, *Phys. Scr.*, **83**, 015301 (2011).

9. Y. Ishikawa, M. J. Vilkas, *Int. J. Quantum Chem.*, **90**, 410–418 (2002).

10. E. Biémont, A. El Himdy, H. P. Garnir, *J. Quant. Spectrosc. Radiat. Transfer*, **43**, 437–443 (1990).

11. Z.-B. Chen, K. Wang, *At. Data Nucl. Data Tables*, **114**, 61–261 (2017).

12. K. B. Fournier, *At. Data Nucl. Data Tables*, **68**, 1–48 (1998).

13. S. B. Utter, P. Beiersdorfer, E. Träbert, *Can. J. Phys.*, **80**, 1503–1515 (2002).

14. Yu. Ralchenko, J. Reader, J. M. Pomeroy, J. N. Tan, J. D. Gillaspy, *J. Phys. B: At. Mol. Opt. Phys.*, **40**, 3861–3875 (2007).

15. U. Litzén and X. Zeng, *J. Phys. B: At. Mol. Opt. Phys.*, **24**, L45 (1991).

16. A. G. Trigueiros, C. J. B. Pagan, S.-G. Pettersson, J. G. Reyna Almandos, *Phys. Rev. A*, **40**, 3911–3914 (1989).

17. I. N. Draganić, Yu. Ralchenko, J. Reader, J. D. Gillaspy, J. N. Tan, J. M. Pomeroy, S. M. Brewer, D. Osin, *J. Phys. B: At. Mol. Opt. Phys.*, **44**, 025001 (2011).

18. C. Biedermann, R. Radtke, G. Fußann, J. L. Schwob, P. Mandelbaum, *Nucl. Instrum. Methods Phys. Res. B*, **235**, 126–130 (2005).

19. C. Suzuki, T. Kato, H. A. Sakaue, D. Kato, K. Sato, N. Tamura, S. Sudo,N. Yamamoto, H. Tanuma, H. Ohashi, R. D'Arcy, G. O'Sullivan, *J. Phys. B: At. Mol. Opt. Phys.*, **43**, 074027 (2010).

20. T. Shirai, J. Sugar, A. Musgrove, W. L. Wiese, Spectral Data for Highly Ionized Atoms: Ti, V, Cr, Mn, Fe, Co, Ni, Cu, Kr and Mo, *J. Phys. Chem. Ref. Data*, AIP Press, Melville, New York (2000); http://physics.nist.gov/PhysRefData/ASD/lines_form.html

21. J. P. Desclaux, *Comput. Phys. Commun.*, **9**, 31–45 (1975).

22. J. P. Desclaux, P. Indelicato, MCDFGME, *a MultiConfiguration Dirac Fock and General Matrix Elements Program, release 2005*; http://dirac.spectro.jussieu.fr/mcdf.

23. E. Träbert. *Phys. Scr.*, **T144**, 014004 (2011).